Fig. S1

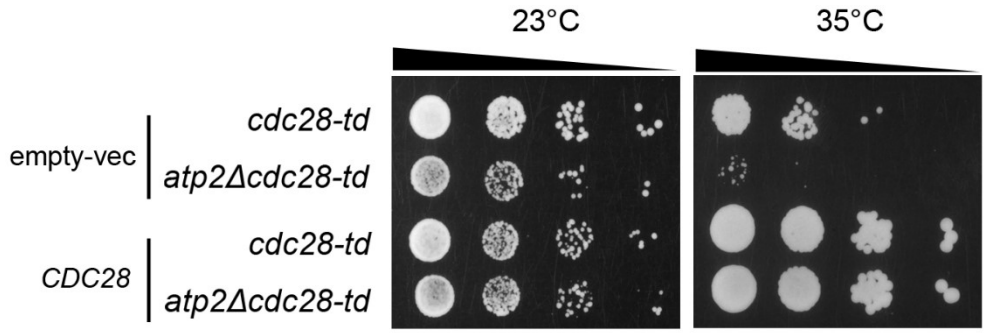

Fig. S1. Reintroducing wt Cdc28 restored the *atp2Δcdc28td* mutant growth at semi-permissive temperature. Growth analysis of *cdc28td* and *atp2Δcdc28td* transformed with empty-vector (YCP50) or the YCP50-derived pHLP183 vector (expressing *CDC28* from its natural promoter; a gift from Mark C. Hall (Hall, Jeong et al., 2008)). Cells were spotted in serial dilutions and grown at indicated semi-permissive temperatures. A representative result is shown (n=3).

Fig. S2

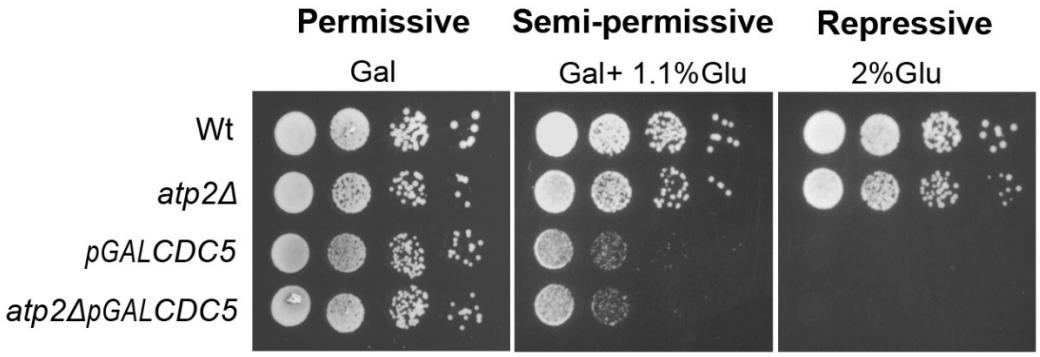

Fig. S2. *ATP2* does not genetically interact with the polo-like kinase encoding gene *CDC5*. Growth analysis of wt, *atp2*Δ, *pGAL1-CDC5* and *atp2*Δ*pGAL1-CDC5* strains. *CDC5* was placed under the control of *GAL1* promoter and partially or completely downregulated by growing the cells in the presence of the indicated concentrations of glucose. *CDC5* was placed under the control of the *GAL1* promoter by integrating the plasmid pFA6a-KanMX6-PGAL1-3HA into the wt and *atp2*Δ genomes upstream of *CDC5* (Longtine, McKenzie et al., 1998). Cells were spotted in fourfold serial dilutions. A representative image is shown (n=3).

Fig. S3

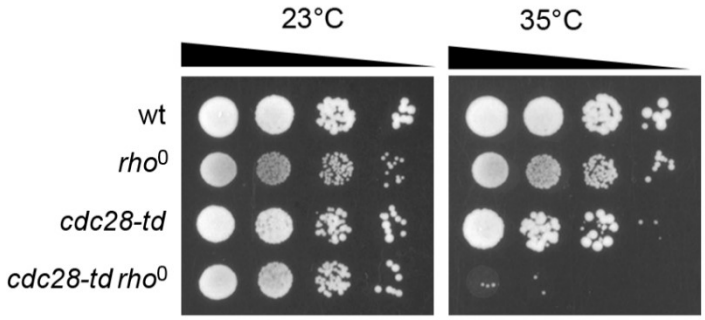

Fig. S3. Ablating mitochondrial DNA in a strain carrying the *cdc28-td* allele aggravates defective growth at semi-permissive temperature. Growth analysis of wt, rho^0, *cdc28td* and rho^0*cdc28td* spotted in serial dilutions and grown at permissive and semi-permissive temperatures. A representative result is shown (n=3). To generate *rho0* strains, cells were grown to saturation twice in liquid YPD medium plus ethidium bromide (25 µg/ml). Individual colonies were selected for growth defects on YPG plates and loss of mtDNA was confirmed by 4′,6-diamidino-2-phenylindole (DAPI) staining.

Fig. S4

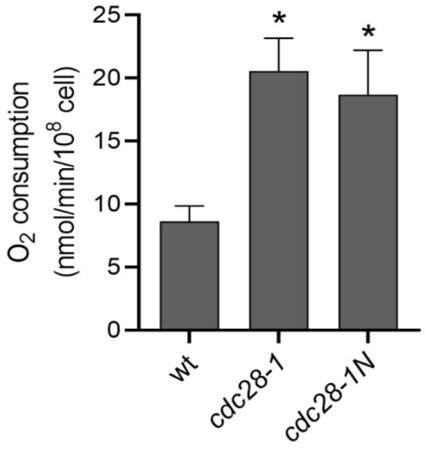

Fig. S4. Respiratory rate is increased in *cdc28-1* and *cdc28-1N* mutants at restrictive temperature. The basal respiratory rate was determined by measuring oxygen consumption in whole cells from glucose grown mid-log phase cultures at the restrictive temperature. Values are the mean ± SD (n =4); *, $p < 0.05$; one-way ANOVA.

Fig. S5

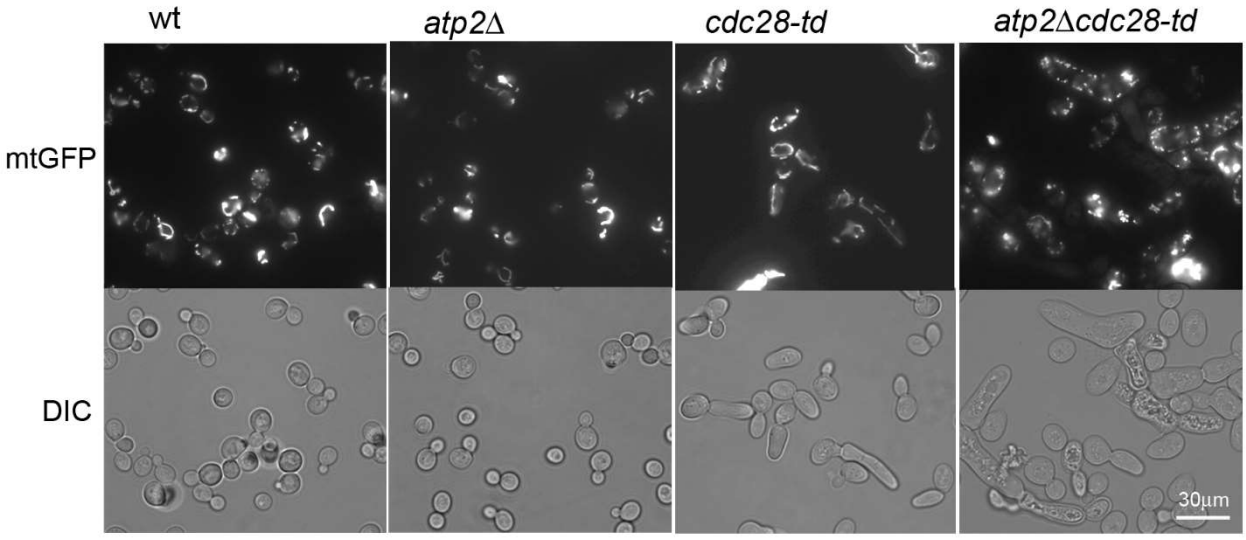

Fig. S5. Mitochondrial morphology is disrupted in double *atp2Δcdc28-td* strain. (A) Indicated yeast cells expressing mtGFP were analyzed by fluorescence microscopy. Representative images are DIC merged with maximum intensity projections of z stacks. Images were acquired by epifluorescence in a Zeiss Axio Imager Z1 microscope fitted with Nomarski optics with an Axiocam MR3.0 camera and Axiovision 4.7 software.

Fig. S6

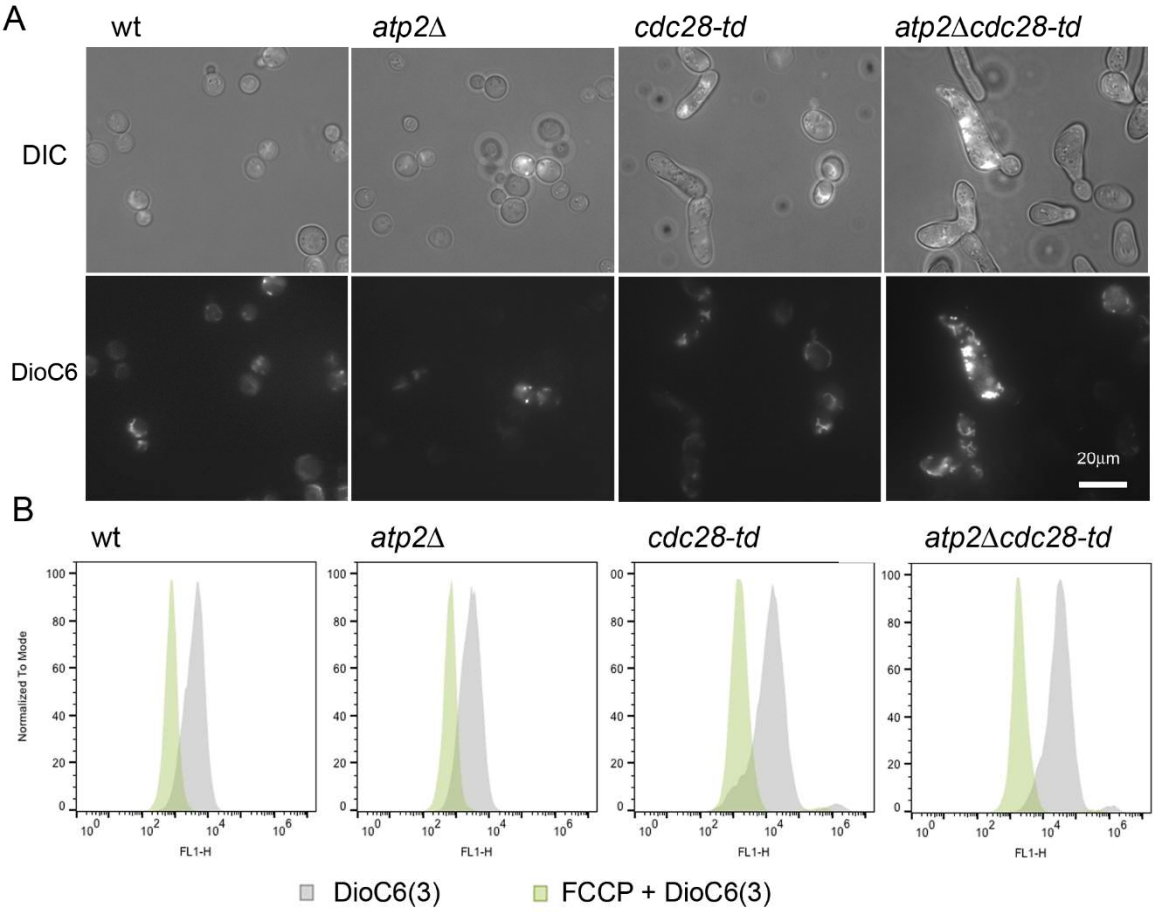

Fig. S6. Mitochondrial membrane potential is altered in double *atp2Δcdc28-td* mutant. (A) The mitochondrial localization of the fluorochrome DioC6(3) was checked by fluorescence microscopy. Representative images are DIC merged with maximum intensity projections of z stacks of DioC6(3) staining. (B) Addition of the FCCP protonophor, which dissipates the $\Delta\psi m$, lead to a substantial reduction of the $DiOC_6$ uptake for all strains.

Fig. S7

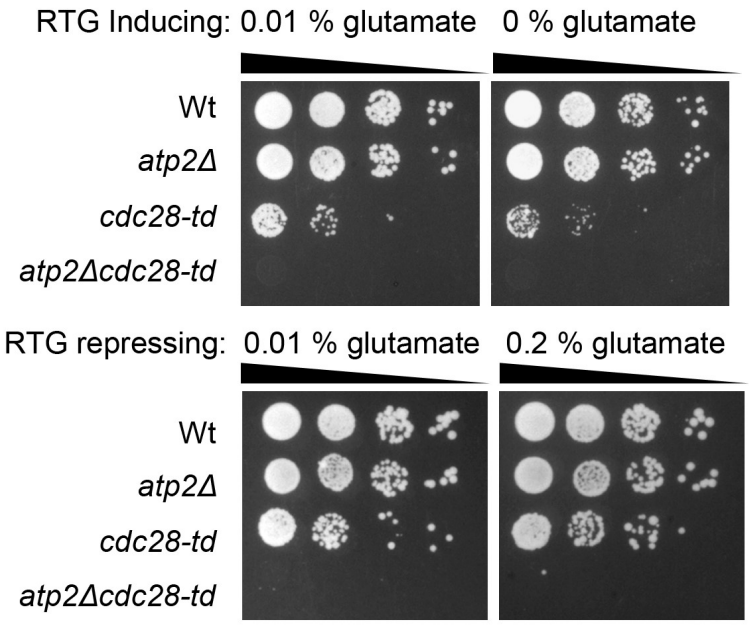

Fig. S7. Absence or excess of glutamate, a repressor of RTG-dependent gene expression, do not supress the growth defects of the *atp2Δcdc28-td* strain. Serial dilutions of indicated strains after growth at the semi-permissive temperature (35 ºC) in minimal media containing 0.01% glutamate (control), lacking or containing 0.2% glutamate.

Fig. S8

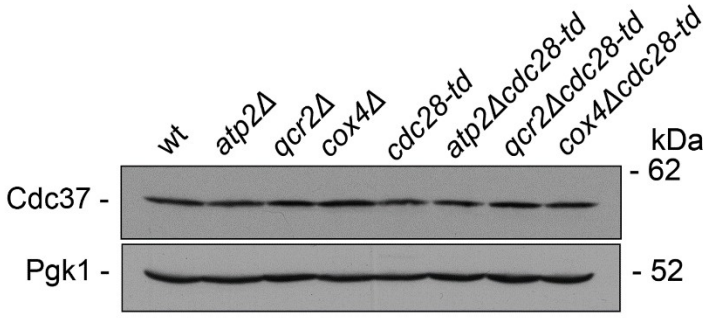

Fig. S8. Cdc37 levels are unchanged in OXPHOS mutants, single or in combination with *cdc28-td*. Western blot analysis of Cdc37 steady-state protein levels in indicated strains cultures at semi-permissive temperature of 26 ºC. Pgk1 is shown as loading control. A representative blot is shown (n=2).

Fig. S9

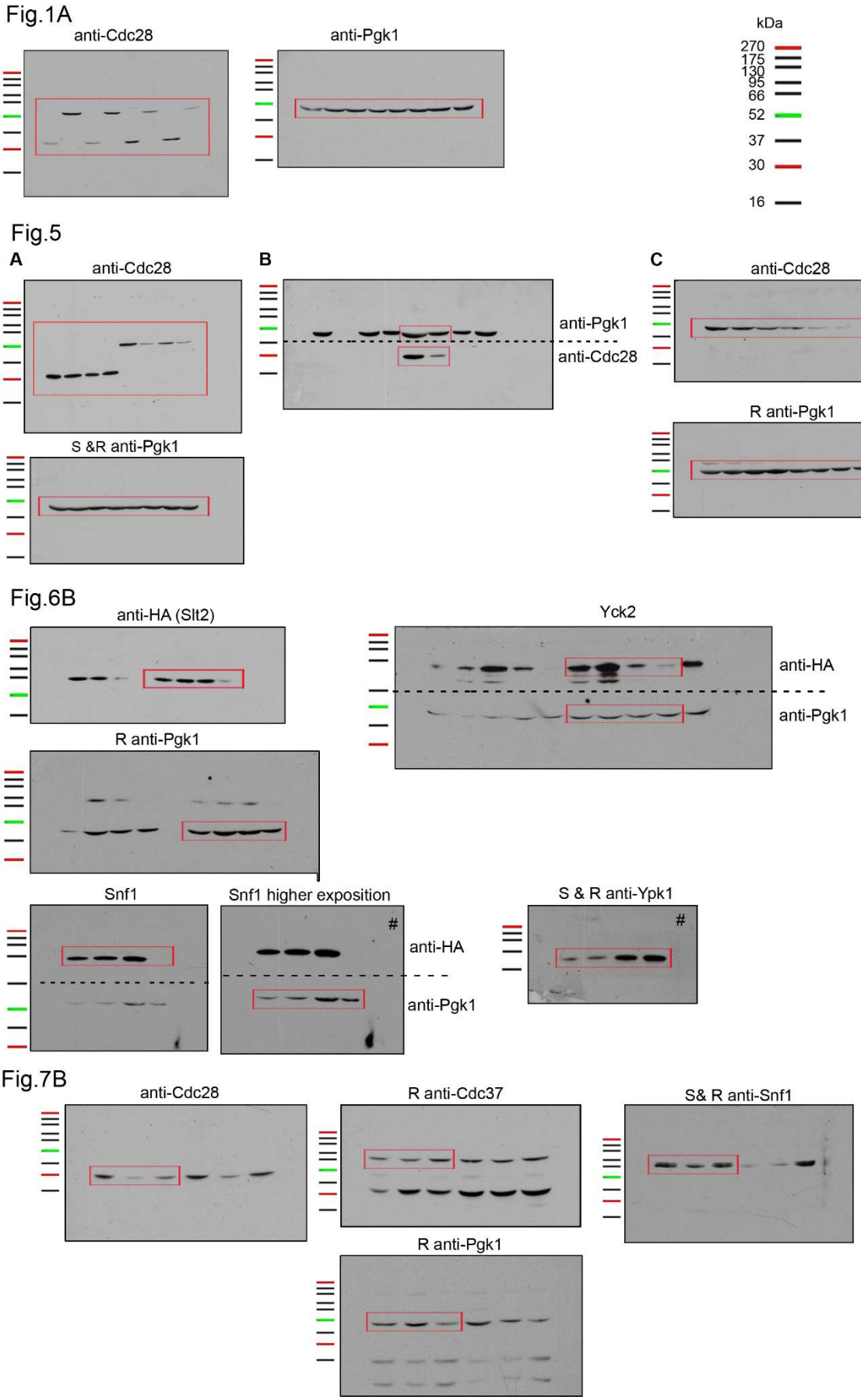

Fig. S9. Blot transparency. Full-length western blots with indicated antibodies and molecular weight markers are shown for bands displayed in Figures 1, 5-7. Protein Ladder: GRS Protein Marker MultiColour PLUS. Red rectangles are used to highlight where the bands were taken from. R indicates Reprobing; S & R indicates Stripping before Reprobing. Dotted line indicates where the membranes were cut for antibody incubation and re-aligned for imaging.

References

Hall MC, Jeong DE, Henderson JT, Choi E, Bremmer SC, Iliuk AB, Charbonneau H (2008) Cdc28 and Cdc14 control stability of the anaphase-promoting complex inhibitor Acm1. *J Biol Chem* 283: 10396-407

Longtine MS, McKenzie A, 3rd, Demarini DJ, Shah NG, Wach A, Brachat A, Philippsen P, Pringle JR (1998) Additional modules for versatile and economical PCR-based gene deletion and modification in Saccharomyces cerevisiae. *Yeast* 14: 953-61

Table S1. *S. cerevisiae* strains used in this study.

Strain	Genotype	Source
BY4741	Mat *a*; *his3Δ1 leu2Δ0 met15Δ0 ura3Δ0*	EUROSCARF
atp2Δ	BY4741; *atp2Δ::HIS3MX6*	Lab collection
cdc28-td	BY4741; *cdc28-td:KanMX4*	EUROSCARF [1]
atp2Δcdc28-td	BY4741; *atp2Δ::HIS3MX6 cdc28-td:KanMX4*	This study
cdc28-1	BY4741; *cdc28-1:KanMX4*	EUROSCARF [1]
atp2Δcdc28-1	BY4741; *atp2Δ::HIS3MX6 cdc28-1:KanMX4*	This study
cdc28-4	BY4741; *cdc28-4:KanMX4*	EUROSCARF [1]
atp2Δcdc28-4	BY4741; *atp2Δ::HIS3MX6 cdc28-4:KanMX4*	This study
cdc28-1N	BY4741; *cdc28-1N:KanMX4*	This study
atp2Δcdc28-1N	BY4741; *atp2Δ::HIS3MX6 cdc28-1N:KanMX4*	This study
cox4Δ	BY4741; *cox4Δ::HIS3MX6*	This study
cox4Δcdc28-td	BY4741; *cox4Δ::HIS3MX6 cdc28-td:KanMX4*	This study
qcr2Δ	BY4741; *qcr2Δ::HIS3MX6*	This study
qcr2Δcdc28-td	BY4741; *qcr2Δ::HIS3MX6 cdc28-td:KanMX4*	This study
atp1Δ	BY4741; *atp1Δ::HIS3MX6*	This study
atp1Δcdc28-td	BY4741; *atp1Δ::HIS3MX6 cdc28-td:KanMX4*	This study
atp4Δ	BY4741; *atp4Δ::HIS3MX6*	This study
atp4Δcdc28-td	BY4741; *atp4Δ::HIS3MX6 cdc28-td:KanMX4*	This study
rtg3Δ	BY4741; *rtg3Δ::URA3MX6*	This study
atp2Δrtg3Δcdc28-td	BY4741; *atp2Δ::HIS3MX rtg3Δ::URA3MX6 cdc28-td:KanMX4*	This study
cdc20-1	BY4741; *cdc20-1:KanMX4*	EUROSCARF [1]
atp2Δcdc20-1	BY4741; *atp2Δ::HIS3MX6 cdc20-1:KanMX4*	This study
ipl1-1	BY4741; *ipl1-1:KanMX4*	EUROSCARF [1]
atp2Δ ipl1-1	BY4741; *atp2Δ::HIS3MX6 ipl1-1:KanMX4*	This study
rho^0 *CIT2-LacZ*	BY4741; rho^0 *CIT2-LacZ:CIT2*	This study
CIT2-LacZ	BY4741; *CIT2-LacZ:CIT2*	This study
cdc28-td CIT2-LacZ	BY4741; *cdc28-td; CIT2-LacZ:CIT2*	This study
atp2Δcdc28-td CIT2-LacZ	BY4741; *atp2Δcdc28-td*; *CIT2-LacZ:CIT2*	This study
cdc28-1 CIT2-LacZ	BY4741; *cdc28-1; CIT2-LacZ:CIT2*	This study
atp2Δcdc28-1 CIT2-LacZ	BY4741; *atp2Δcdc28-1*; *CIT2-LacZ:CIT2*	This study
cdc28-1N CIT2-LacZ	BY4741; *cdc28-1N; CIT2-LacZ:CIT2*	This study
atp2Δcdc28-1N CIT2-LacZ	BY4741; *atp2Δcdc28-1N*; *CIT2-LacZ:CIT2*	This study
DH211	TM141 *cdc37Δ::HIS3* [Ycplac111 CDC37-HA]	[2]
DH212	TM141 *cdc37Δ::HIS3* [Ycplac111 cdc37-S14A-HA]	[2]

References

[1] Li, Z.J., et al., Nature Biotechnology, 2011. **29**(4): p. 361-U105.
[2] Hawle, P., et al.. Eukaryotic Cell, 2007. **6**(3): p. 521-532.